Highlight Review

Propylene Oxide Synthesis and Selective Oxidation over Supported Metal Oxide Photocatalysts with Molecular Oxygen

Fumiaki Amano and Tsunehiro Tanaka*

(Received February 15, 2006; CL-068002)

Abstract

Recent progress of photocatalytic epoxidation of propylene with molecular oxygen is reviewed. Highly dispersed metal oxide photocatalysts, such as silica-supported V_2O_5, Nb_2O_5, and TiO_2 with low loading, promote steady-state propylene oxide formation with high selectivity (>40%). The isolated tetrahedrally-coordinated species in the ligand-to-metal charge-transferred state is the photocatalytic active site. The photo-induced hole center localized on the lattice oxygen plays a significant role for the photocatalytic epoxidation. In the case of isolated TiO_4 tetrahedra on silica, an electrophilic oxygen species is generated by the reaction between the hole center and molecular oxygen. The addition of alkali ions to surface VO_4 tetrahedra improves the photocatalytic epoxidation ability of V_2O_5/SiO_2 with low loading. The key step in the selective photocatalytic oxidation over isolated VO_4 tetrahedra is the electron transfer from a hydrocarbon to the photo-induced hole center on the lattice oxygen, which is inserted in the photogenerated products.

1. Introduction

The use of solar energy as a reagent is an economically advantageous process for chemical conversion. A great deal of attention has been devoted to photocatalytic systems for activation of molecular oxygen in order to achieve selective oxygenation of organic molecules.[1,2] There are two types of photocatalysts as shown in Figure 1, typically divided to inorganic semiconductor photocatalyst and organic photosensitizer photocatalyst.[3]

When metal oxide particles as semiconductor absorb photoenergies larger than the band gap, the photo-excited electrons and holes are produced in the conduction band and the valence band, respectively. An efficient charge separation promotes the chemical reactions competing with a recombination of the electrons and the holes. In the case of photosensitizer, an electron in the highest occupied molecular orbital (HOMO) is transferred to the lowest unoccupied molecular orbital (LUMO). The electronically excited state can act as stronger electron donor and accepter than the ground state. The long-lived triplet state via intersystem crossing from the singlet state effectively promotes chemical reactions in competition with a radiative back-electron transfer to the ground state.

An attention of recent studies has been concentrated mainly on degradation and mineralization of pollutants using TiO_2 semiconductor photocatalysts. On the irradiated TiO_2 surface, many kinds of active oxygen species and radicals are present simultaneously, which lead to total oxidation of organic molecules to carbon dioxide. Therefore, a control of selective partial oxidation with molecular oxygen is difficult on conventional semiconductor photocatalysts.

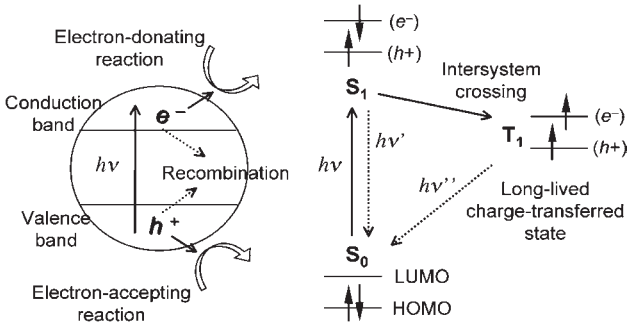

Figure 1. Semiconductor and photosensitizer photocatalysts.

Tanaka et al. found that highly dispersed niobium oxide species on silica are active for photoepoxidation of propylene in the presence of molecular oxygen at room temperature.[4] Propylene oxide (PO) is a great important product in chemical industry. However, direct epoxidation of propylene by molecular oxygen, which is an ideal oxidant from the environmental and economic viewpoints, is difficult due to the high reactivity of the allylic C–H bonds. Recently, indirect epoxidation method by in situ generation of H_2O_2 from O_2 has been reported over titanosilicate-supported noble metals, although it is necessary to improve the utilization efficiency of the co-feeding hydrogen and the production rate of PO.[5] The excellent work by Yoshida and co-workers shows that many kinds of highly dispersed metal oxide species on silica exhibit ability to PO formation in the photooxidation of propylene using O_2.[6] Such a direct photoepoxidation of lower alkenes has not been reported in any other photosystems except for the highly dispersed metal oxide photocatalysts. In the present paper, the photocatalytic epoxidation of propylene with molecular oxygen over silica-supported metal oxides, especially over V_2O_5/SiO_2, are reviewed.

2. Photoepoxidation of Propylene over Supported Metal Oxide

Strategies for the design of a photocatalyst for partial oxidation are to control the number and the kinds of active oxygen species and create a catalytic site for a selective reaction with the reactant molecules. An atomically dispersed metal oxide species on silica would be recognized as a mononuclear complex attached to the surface. This species exhibits the property of pho-

*Dr. Fumiaki Amano, Prof. Tsunehiro Tanaka**
Department of Molecular Engineering, Graduate School of Engineering, Kyoto University, Kyoto Daigaku Katsura, Nishikyo-ku, Kyoto 615-8510
E-mail: tanakat@moleng.kyoto-u.ac.jp

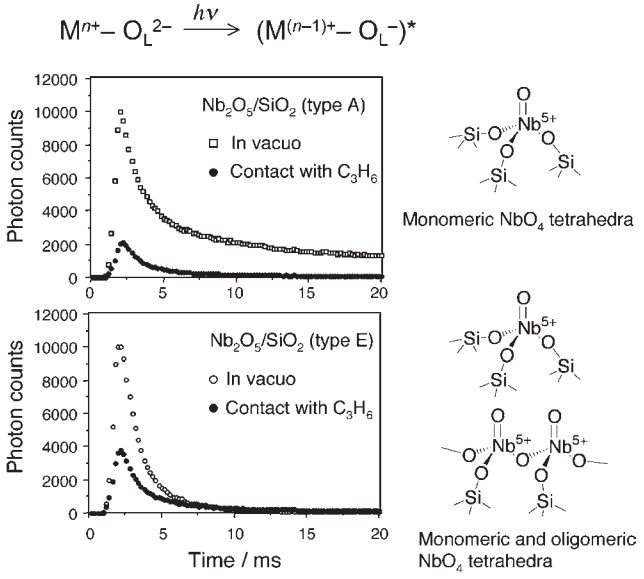

Figure 2. Phosphorescence emission decay curves of Nb_2O_5/SiO_2 prepared by an equilibrium adsorption method (type A) and a conventional evaporation to dryness method (type E).

tosensitizer photocatalyst rather than semiconductor photocatalyst. Photoexcitation causes a charge transfer from the oxygen ligand to the metal cation (LMCT transition). Since silica is an insulator, the photo-induced electron and hole are localized on the isolated metal oxide species. This charge-transferred excited state with a hole center trapped on the lattice oxygen and an electron on the metal cation would be favorable for promoting selective reaction, such as partial oxidation.[7]

On the basis of this concept, two types of Nb_2O_5/SiO_2 were prepared by an equilibrium adsorption method (type A, 0.2 wt % as Nb_2O_5) and conventional evaporation to dryness method (type E, 0.1 wt % as Nb_2O_5).[4,8] The type A catalyst contains monomeric NbO_4 tetrahedra, and type E catalyst both monomeric and oligomeric NbO_4 tetrahedra. As shown in the phosphorescence decay curves (Figure 2), type A catalyst exhibits long-lived emission species.[4] By a contact with propylene, the emission was quenched more efficiently for type A than for type E catalyst. This indicates that the monomeric NbO_4 tetrahedra in the excited triplet state preferentially interact with propylene. The type A exhibits higher selectivity and activity for PO formation than the type E catalyst in the photooxidation of propylene with O_2 in a closed circulation reactor.

A series of highly dispersed transition-metal oxides such as TiO_2,[9,10] ZnO,[11] and CrO_3[12] in and on SiO_2, have also been found to promote photoepoxidation of propylene with high selectivity (60% for TiO_2–SiO_2[9,10]). It has been reported that the TiO_2–SiO_2 could be extended to other light alkenes such as ethylene and butenes. In general, the active sites for photoepoxidation exist in an isolated state with tetrahedral coordination.[7] The selectivity in the photooxidation over the highly dispersed metal oxides is significantly different from that over the corresponding metal oxide clusters. The typical semiconducting photocatalysts (TiO_2 and ZnO) predominantly promote the total oxidation to CO_2 in the photocatalytic oxidation of propylene.[13,14] Although trace amounts of PO and propanal were produced at the extremely low conversion level, the unstable products are consecutively

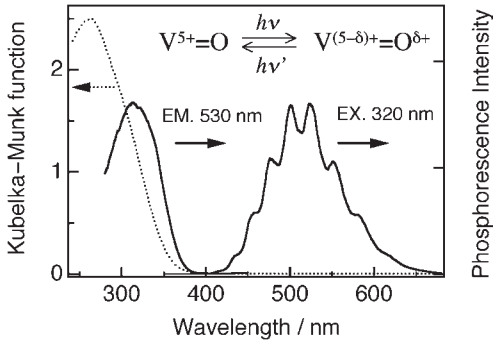

Figure 3. Diffuse reflectance UV–vis spectrum and photoluminescence spectra of 0.5 wt % V_2O_5/SiO_2 at dehydrated state. The phosphorescence excitation and emission spectra were recorded by monitoring at 530 nm and excitation at 320 nm, respectively.

decomposed. In the case of higher alkenes such as 2-hexene, photocatalytic epoxidation was promoted over TiO_2 and Ti-containing SiO_2 using molecular oxygen.[15,16]

♦ 3. Photocatalytic Epoxidation of Propylene over V_2O_5/SiO_2

It is well known that the isolated VO_4 tetrahedra supported on SiO_2 exhibit photoactivity for oxidation from the photoluminescence studies.[17] Figure 3 shows the phosphorescence spectra of the dehydrated V_2O_5/SiO_2 at a liquid nitrogen temperature. The lifetime of the emission was about 10 ms. The vibrational fine structure of the emission is attributed to the stretching of the terminal vanadyl V=O bond[17] or the basal V–O–Si bonds.[18] It is generally accepted that the triplet emission state involves an intersystem crossing from the singlet excited state localized on monooxo-vanadium group. The promotion of an electron into the antibonding orbital of the V=O bond ($n \rightarrow \pi^*$ transition) destabilizes and activates the lattice terminal oxygen that is responsible for the photooxidation of CO (lattice oxygen insertion). Tanaka et al. examined the photooxidation of propylene with molecular oxygen over the V_2O_5/SiO_2.[19b,20] The products were ethanal, propenal, and propanal. However, PO was not detected although the formation of PO had been predicted as a precursor to propanal.[20]

The previous studies on the propylene photooxidation estimated the activity of highly dispersed metal oxide photocatalysts using a closed reactor system.[4,6,9–12,19–21] The long contact time is disadvantage on the decomposition of the unstable intermediates. Moreover, it is unclear that the photo-assisted synthesis of PO is really "catalytic" reaction. Therefore, a flow reactor was adopted instead of a conventional closed reactor.[22–24]

Figure 4 shows the results of the photocatalytic epoxidation of propylene over V_2O_5/SiO_2 with different vanadium loadings. Using a flow system, the selective formation of PO over the isolated VO_4 tetrahedra on silica could be observed for the first time.[22] At 303 K, the conversion rate of propylene was maximized on the 0.1 wt % loaded catalysts (0.01 V-atom nm^{-2}). The selectivity to PO reached 40% and decreased with an increase in the loading amount. The decrease in the propylene conversion is because of a suppression of the desorption of the photogenerated PO from the catalyst surface due to the acid sites, the number of which is linearly increased with the V_2O_5 loading.

Published on the web (Advance View) April 1, 2006; DOI: 10.1246/cl.2006.468

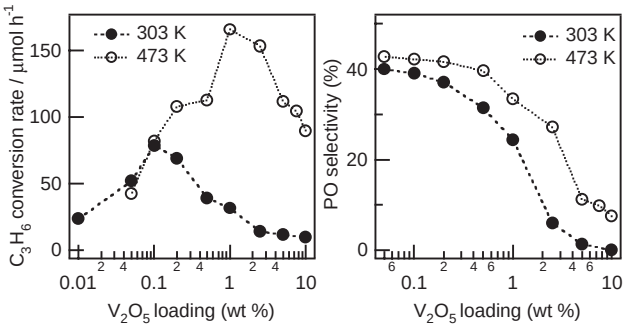

Figure 4. Effect of V_2O_5 loading on the conversion rate of propylene and the selectivity to PO in the photooxidation of C_3H_6 with O_2 over V_2O_5/SiO_2 in a flow reactor. Catalyst 0.3 g. Total flow rate 100 mL min^{-1}. Reactants: 20% C_3H_6, 10% O_2, 70% He. Irradiation $240 < \lambda < 440$ nm. Reaction temperature 303 and 473 K.

By heating the catalysis bed to 473 K during the photooxidation, the conversion rate of propylene was significantly increased at the higher loading region than 0.1 wt %. Up to the loading amount < 2.5 wt %, the samples consist of a monomeric VO_4 tetrahedral species dispersed on SiO_2.[22] Therefore, the isolated $(SiO)_3V{=}O$ species is the photocatalytic active site for PO formation. In the case of highly loaded V_2O_5/SiO_2, propanal was selectively produced instead of PO (the selectivity to propanal on 10 wt % V_2O_5/SiO_2: 40%).[22] This indicates that propanal is formed as a secondary product via PO. The isomerization of PO over vanadium oxide species on SiO_2 has been confirmed under thermal treatment in a closed circulation reactor.[20]

The catalysts, such as Nb_2O_5/SiO_2,[4] MgO/SiO_2,[21] TiO_2/SiO_2,[9,10] ZnO/SiO_2,[11] and CrO_3/SiO_2,[12] have been reported as effective for photoepoxidation of propylene in a closed reactor. Photocatalytic epoxidation of propylene with O_2 at room temperature was investigated over various silica-supported metal oxides with low loading in a flow reactor.[24] Table 1 shows the results of the photocatalytic epoxidation of propylene after 5 h of time on stream. The high PO yield was achieved over the V, Ti, and Nb oxides on silica. Amorphous silica was more effective than FSM-16 for supported Ti and V oxides. The decrease of PO production is presumably because of the acid properties of FSM-16 silica.[25] Bulk TiO_2, semiconductor photocatalyst, promotes the deep oxidation under UV irradiation.

Table 1. Results of photooxidation of C_3H_6 with O_2 at 303 K[a]

Catalyst	Conversion /μmol h^{-1}	PO yield /μmol h^{-1}	Selectivity/%			
			PO	C3[d]	Ethanal	CO_2
TiO_2/SiO_2[b]	36	18	50	12	18	21
V_2O_5/SiO_2[b]	69	26	37	16	37	10
Nb_2O_5/SiO_2[b]	31	12	40	21	20	20
CrO_3/SiO_2[b]	3	1	42	15	21	21
ZnO/SiO_2[b]	3	2	62	n.d.	7	31
MgO/SiO_2[c]	2	1	74	n.d.	trace	27
SiO_2	2	1	73	n.d.	trace	27
TiO_2 (JRC-TIO-4)	67	0	0	6	13	80
TiO_2/FSM-16[b]	19	7	35	14	27	24
V_2O_5/FSM-16[b]	49	4	8	27	40	26

[a]Catalyst 0.3 g, Total flow rate 100 mL min^{-1}, Reactants: 20% C_3H_6, 10% O_2, 70% He, Irradiation $240 < \lambda < 440$ nm, Reaction temperature 303 K. The data were obtained at 300 min on stream. [b]$M/(M + Si) = 0.1$ mol %. The 0.1 mol % $V/(V + Si)$ is corresponding to 0.15 wt % V_2O_5. [c]$Mg/(Mg + Si) = 1.5$ mol %. [d]The C3-oxygenated products: propanal, propenal, and acetone.

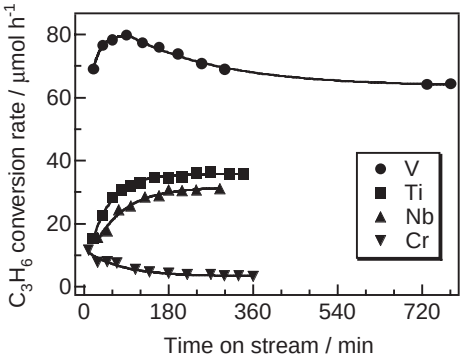

Figure 5. Time course of the photooxidation of C_3H_6 with O_2 over 0.1 mol % TiO_2/SiO_2, V_2O_5/SiO_2, CrO_3/SiO_2, and Nb_2O_5/SiO_2. Catalyst 0.3 g. Total flow rate 100 mL min^{-1}. Reactants: 20% C_3H_6, 10% O_2, 70% He. Irradiation $240 < \lambda < 440$ nm. Reaction temperature 303 K.

Figure 5 shows the time-dependent behavior of the photocatalytic epoxidation of propylene at 303 K. The conversion rate of propylene and the formation rate of PO were increased in the order Nb < Ti < V oxides on silica. The selectivity to PO at steady state was very stable during the reaction. In the case of CrO_3/SiO_2, a gradual deactivation was observed with the course of the photoreaction, although the initial activity was detected.

♦ 4. Mechanism of Photocatalytic Epoxidation

The oxidation state and the coordination environment of the supported Ti, V, and Cr oxide species were determined by diffuse reflectance UV–vis spectroscopy and electron spin resonance (ESR).[24] During the photocatalytic oxidation, the oxidation state of the Ti^{4+} species was not varied. On the other hand, the V^{5+} species was partially reduced to V^{4+}. An isotopic tracer study of the C_3H_6–$^{18}O_2$ reaction suggests the difference of the reaction mechanisms between TiO_2/SiO_2 and V_2O_5/SiO_2.[24] The active oxygen species on TiO_2/SiO_2 is derived from molecular oxygen. On the other hand, the photogenerated products on V_2O_5/SiO_2 incorporate the lattice oxygen of the surface metal oxide species.

Figure 6 shows proposed reaction mechanisms in the photocatalytic epoxidation of propylene. By the ESR and isotropic tracer studies on TiO_2/SiO_2, Yoshida et al. have concluded that the active oxygen species for photoepoxidation of lower alkenes is an electrophilic T-type O_3^- species ($O_2^{\bullet+}$ adsorbed on O_L^{2-}) generated by the reaction between an O_2 molecule and a photoformed hole center on the lattice oxygen (O_L^-).[10] This electron-deficient oxygen moiety could preferably react with electron rich part of alkenes to produce the epoxides. The photogenerated PO includes nearly 100% of ^{18}O-oxygen in the C_3H_6–$^{18}O_2$ reaction over monomeric TiO_4 tetrahedra in silica.[10] The photo-induced electron in Ti^{3+} reacts with O_2 to form $O_2^{\bullet-}$ species, which could not activate propylene by itself. In the absence of oxygen, allyl radical or methyl radical are formed by the reaction between O_L^- and propylene. The radical formation resulted in un-

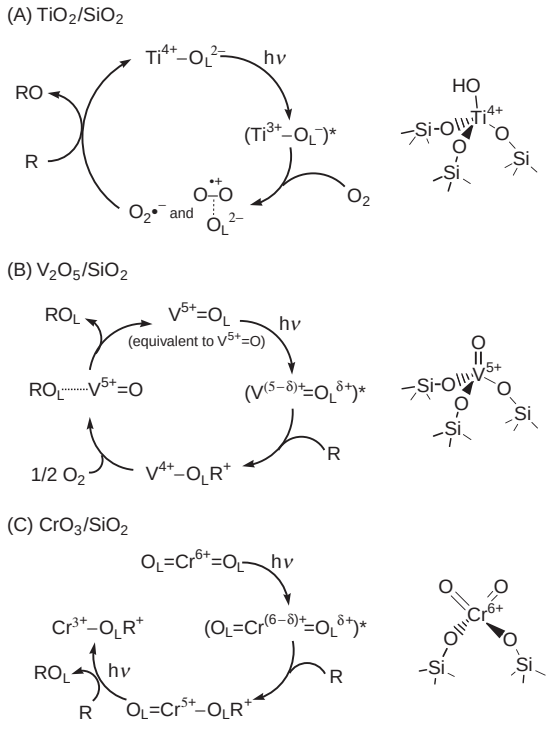

Figure 6. Proposed reaction mechanisms in the C_3H_6 photooxidation with O_2 over (A) TiO_2/SiO_2, (B) V_2O_5/SiO_2, and (C) CrO_3/SiO_2, where R is propylene and RO is propylene oxide. The O_L indicates oxygen atom originated from lattice oxygen.

desirable side reactions. Recently, Shiraishi et al. found that an addition of acetonitrile suppresses the electron transfer from alkenes to hole center on Ti-containing silica and improves the epoxide selectivity in the photooxidation of higher alkenes.[16]

In the case of V_2O_5/SiO_2, the photo-activated oxo ligand is the active oxygen species for PO production.[24] The lattice oxygen in the excited triplet state, $(V^{(5-\delta)+}=O^{\delta+})^*$, is considered to exhibit electrophilic character, which attacks the double bond in propylene. On the contrary to TiO_2/SiO_2, the electron transfer from propylene to the hole center would form an epoxide-like intermediate attached to the lattice oxygen. The V^{4+} cation trapping an electron will be oxidized by oxygen molecule.

Figure 7 shows ESR spectra of CrO_3/SiO_2 catalyst.[24] When the sample was irradiated with 20 Torr of C_3H_6 and 10 Torr of O_2 for 1 min, axial symmetric γ-signal due to $Cr^{5+}(d^1)$ was immediately increased and gradually decreased with an increase of broad δ-signal characterized by a positive lobe, which is assigned to isolated $Cr^{3+}(d^3)$ species. This indicates that the Cr^{6+} species was successively reduced to photo-inactive species such as Cr^{5+} and Cr^{3+}. The reduced species resisted to the reoxidation by molecular oxygen even at 673 K. Although the CrO_3/SiO_2 is attractive material for photooxidation using visible light,[12,26] the photoreaction is stoichiometric rather than photocatalytic (Figure 6c). Since there is an initial activity, the photo-activated lattice oxygen has capability for propylene oxidation.

In the case of the monooxo $(SiO)_3V{=}O$ and dioxo $(SiO)_2Cr(=O)_2$ species, a photo-induced hole center on the lattice oxygen directly reacts with propylene. On the contrary, a photo-induced hole center on the mono-hydroxyl $(SiO)_3Ti$-OH

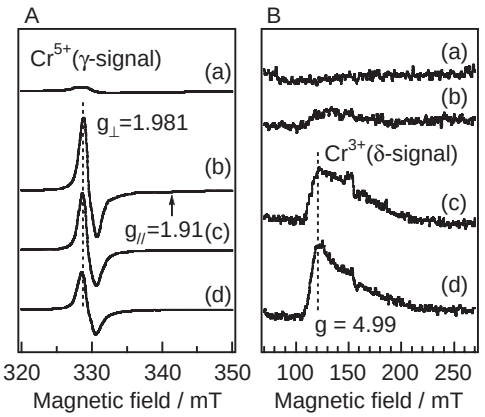

Figure 7. ESR spectra of 0.1 mol % CrO_3/SiO_2 at room temperature (A) and 123 K (B): The spectra were recorded after calcination and outgassing at 673 K (a), irradiation in the presence of 20 Torr C_3H_6 and 10 Torr O_2 for 1 min (b), 10 min (c), and 30 min (d) at room temperature and outgassing.

species activates O_2 to electrophilic oxygen species (T-type O_3^-). It is suggested that the kinds of the terminal ligand (hydroxyl or oxo) of the tetrahedrally coordinated metal oxides on silica decide the kinds of active oxygen species in the photocatalytic oxidation.

♦ 5. Modification of Photocatalytic Center of V_2O_5/SiO_2

Among the highly dispersed metal oxides, the vanadium oxide species anchored on silica shows the highest photocatalytic activity.[24] Moreover, it is possible to enhance the photooxidation ability of V_2O_5/SiO_2 by an alkali ion addition.[27,28] The alkali ion interacts to the terminal oxo of the monomeric VO_4 tetrahedron on silica. Amano and Tanaka tried the modification of the electronic state of the photocatalytic center, the photo-excited lattice oxygen, by an alkali ion addition in order to achieve further improvement of the PO formation rate.[23] The photooxidation of propylene with O_2 was investigated over alkali-ion-modified V_2O_5/SiO_2 at low vanadium loading. The addition of Rb^+ ions to 0.5 wt % V_2O_5/SiO_2 resulted in the great improvement of the formation rate of PO.[23] Alkali ions of Li^+, Na^+, K^+, and Cs^+ gave the similar effect upon the photocatalysis. The photocatalytic performances of Rb-ion-modified V_2O_5/SiO_2 are summarized in Table 2. The propylene conversion and the PO selectivity over Rb-ion-modified V_2O_5/SiO_2 (Rb/V molar ratio = 0.5–3.0) are higher than that of non-modified V_2O_5/SiO_2. The photocatalytic activity was significantly enhanced when the Rb/V value varied from 0.5 through 1.0. Because the pH value of the solution used for catalyst preparation is high, the specific surface area of Rb-ion-modified V_2O_5/SiO_2 was reduced with an increase in the amount of Rb addition. The higher Rb-ion-addition drastically decreased the PO formation rate due to an enhancement of non-selective oxidation to CO_2.

Figure 8 shows diffuse reflectance UV–vis spectra of Rb-ion-modified V_2O_5/SiO_2.[23] The color of V_2O_5/SiO_2 was yellowish green at hydrated state. The band observed around 400 nm is assigned to the LMCT transitions of the V_2O_5-like polymerized species. It is known that the tetrahedral VO_4 monomers on silica at dehydrated state are changed to square pyrami-

Table 2. Results of photooxidation of C_3H_6 with O_2 over Rb-ion-modified 0.5 wt % V_2O_5/SiO_2[a]

Rb/V	S_{BET}[b] /$m^2\ g^{-1}$	TOS[c] /min	Conversion /%	Selectivity/%			
				PO	C3[d]	Ethanal	CO_2
0	588	180	0.4	14	19	52	15
0.5	510	60	0.6	28	8	31	33
1	485	60	1.4	31	6	16	47
1.5	348	60	1.6	31	7	15	47
		600	1.4	28	8	15	49
3	296	60	1.5	19	5	10	66
6	191	60	1.0	9	5	6	80

[a]Catalyst 0.3 g. Total flow rate 25 mL min^{-1}. Reactants: 20% C_3H_6, 10% O_2, 70% He. Irradiation $240 < \lambda < 440$ nm. Reaction temperature 303 K. [b]BET specific surface area. [c]Time on stream. [d]The C3-oxygenated products: propanal, propenal, and acetone.

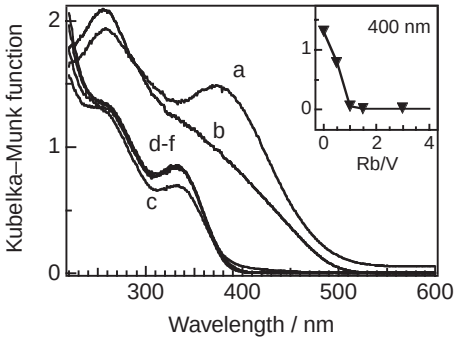

Figure 8. Diffuse reflectance UV–vis spectra of Rb-ion-modified V_2O_5/SiO_2 at hydrated state, V_2O_5 loading 0.5 wt %, Rb/V molar ratio = 0 (a), 0.5 (b), 1.0 (c), 1.5 (d), 3.0 (e), and 6.0 (f). The inset reports the Kubelka–Munk function at 400 nm on the Rb/V molar ratio.

dal VO_5 polymers by water adsorption.[29,30] This band at visible region decreased with the addition of Rb^+ ions and fully disappeared when the Rb/V value of the samples was more than 1.0. This disappearance is due to the suppression of the aggregation of isolated species into square pyramidal polymers under hydrated conditions.[31] The Rb/V value of 1.0 indicates a presence of one-to-one interaction between Rb ion and vanadium ion. Since the conversion of propylene was significantly enhanced at Rb/V value more than 1.0 (Table 2), it was concluded that the alkali ion addition modifies the character of the lattice oxygen of the photocatalytic active center resulting in the creation of one-to-one interacting $RbVO_4$ species for photocatalytic PO synthesis.

♦ 6. Selective Photooxidation over Supported Metal Oxide Photocatalysts

The highly dispersed vanadium oxide species promotes the selective photooxidation of alkanes as well as alkenes with O_2.[28,32,33] Gas-phase selective oxidation of light alkanes is important for the usage of natural gas and liquefied petroleum gas. Tanaka et al. have reported that alkali-ion-modified V_2O_5/SiO_2 is available for selective photocatalytic oxidation of propane and butanes at room temperature.[28] At elevated reaction temperature, 493 K, Wada et al. reported the selective photo-

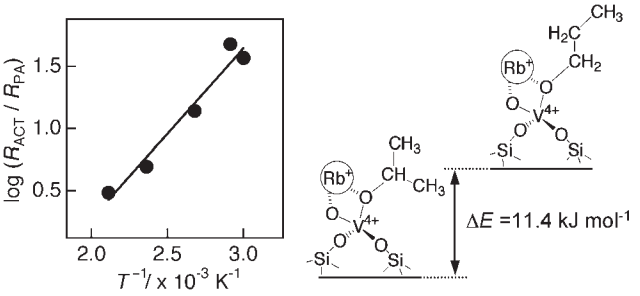

Figure 9. Logarithm plots of the formation ratio of acetone (ACT) to propanal (PA) against the reciprocal of the reaction temperature in photooxidation of propane over Rb-ion-modified V_2O_5/SiO_2.

assisted oxidation of methane to formaldehyde using V_2O_5/SiO_2 photocatalyst.[32] In the case of liquid-phase reaction, silica-supported vanadium oxide is not effective due to the leaching, and V_2O_5/Al_2O_2 exhibits high photocatalytic activity for partial oxidation of hydrocarbons such as cyclohexane in the presence of O_2 at room temperature.[33]

The photocatalytic oxidation mechanism has been investigated for acetone formation from propane.[34,35] The photocatalyst system with Rb-ion-modified V_2O_5/SiO_2 can be operated without deactivation at a high rate of the acetone production in a flow reactor.[36] The active oxygen species is not derived from molecular oxygen but from the lattice oxygen of the VO_4 species interacted with Rb ion.[34] The kinetic analysis demonstrated that the rate-determining step is the reaction of propane with the photo-induced hole center on the lattice oxygen of the Rb-ion-modified VO_4 species to yield the vanadium isopropoxide species.[35] Heating the photocatalyst bed drastically enhanced not only the yield of acetone but also the yield of propanal that is a minor product in the photooxidation at 333 K. Figure 9 shows the logarithm plots of the formation ratio of acetone to propanal (R_{ACT}/R_{PA}) against the reciprocal of the reaction temperature in the photooxidation of propane.[35] A linear relationship suggested that the formation ratio of the precursor into acetone to the precursor into propanal obeys Boltzmann's distribution of the stabilizing energy difference between the precursors, ΔE. The ratio is expressed as follows.

$$\frac{R_{ACT}}{R_{PA}} = \exp\left(\frac{\Delta E}{RT}\right), \quad (1)$$

where R is the gas constant and T is the reaction temperature. The precursors to acetone and propanal are assumed to be an vanadium isopropoxide-like intermediate and an vanadium *n*-propoxide-like intermediate, respectively. The stabilizing energy difference was estimated to be 11.4 kJ mol^{-1} by a slope of Figure 9, which is nearly consistent with the result of DFT calculation of the assuming intermediates (14.1 kJ mol^{-1}).[35] Therefore, it is concluded that the product distribution of the photo-assisted oxidation of propane is described by the stabilization energy difference of the photo-adsorbed propane species that is attached to the lattice oxygen of vanadium species.

♦ 7. Summary

V_2O_5/SiO_2 and alkali-ion-modified V_2O_5/SiO_2 were found to be promising photocatalysts for PO formation in the photooxidation of propylene with O_2 and TiO_2/SiO_2 exhibits excellent

selectivity to PO at fairly high conversion. In the case of V_2O_5-based catalysts, the active oxygen is the lattice oxygen while in the case of TiO_2-based catalysts, it is adsorbed molecular oxygen. However, interestingly, both of the active oxygen species are electrophilic, suggesting that a key step is the electron transfer from a hydrocarbon to an active oxygen species as a photo-induced hole center. As shown in the present review, the kinds and the property of the active oxygen species can be controlled over highly dispersed metal oxide photocatalysts for selective partial oxidation.

References

1 A. Maldotti, A. Molinari, R. Amadelli, *Chem. Rev.* **2002**, *102*, 3811.
2 J. Wahlen, D. E. De Vos, P. A. Jacobs, P. L. Alsters, *Adv. Synth. Catal.* **2004**, *346*, 152.
3 A. Corma, H. Garcia, *Chem. Commun.* **2004**, 1443.
4 T. Tanaka, H. Nojima, H. Yoshida, H. Nakagawa, T. Funabiki, S. Yoshida, *Catal. Today* **1993**, *16*, 297.
5 J. R. Monnier, *Appl. Catal., A* **2001**, *221*, 73.
6 H. Yoshida, C. Murata, T. Hattori, *J. Catal.* **2000**, *194*, 364.
7 H. Yoshida, *Curr. Opin. Solid State Mater. Sci.* **2003**, *7*, 435.
8 H. Yoshida, T. Tanaka, T. Yoshida, T. Funabiki, S. Yoshida, *Catal. Today* **1996**, *28*, 79.
9 H. Yoshida, C. Murata, T. Hattori, *Chem. Commun.* **1999**, 1551.
10 a) C. Murata, H. Yoshida, J. Kumagai, T. Hattori, *J. Phys. Chem. B* **2003**, *107*, 4364. b) C. Murata, T. Hattori, H. Yoshida, *J. Catal.* **2005**, *231*, 292.
11 a) H. Yoshida, C. Murata, T. Hattori, *Chem. Lett.* **1999**, 901. b) H. Yoshida, T. Shimizu, C. Murata, T. Hattori, *J. Catal.* **2003**, *220*, 226.
12 C. Murata, H. Yoshida, T. Hattori, *Chem. Commun.* **2001**, 2412.
13 P. Pichat, J. M. Herrmann, J. Disdler, M. N. Mozzanega, *J. Phys. Chem.* **1979**, *83*, 3122.
14 K. Wada, K. Yoshida, Y. Watanabe, T. Mitsudo, *J. Chem. Soc., Faraday Trans.* **1996**, *92*, 685.
15 a) T. Ohno, K. Nakabeya, M. Matsumura, *J. Catal.* **1998**, *176*, 76. b) T. Ohno, T. Kigoshi, K. Nakabeya, M. Matsumura, *Chem. Lett.* **1998**, 877.
16 Y. Shiraishi, M. Morishita, T. Hirai, *Chem. Commun.* **2005**, 5977.
17 a) A. M. Gritscov, V. A. Shvets, V. B. Kazansky, *Chem. Phys. Lett.* **1975**, *35*, 511. b) M. Anpo, I. Tanahashi, Y. Kubokawa, *J. Phys. Chem.* **1980**, *84*, 3440. c) S. Yoshida, Y. Matsumura, S. Noda, T. Funabiki, *J. Chem. Soc., Faraday Trans.* **1981**, *77*, 2237.
18 a) K. Tran, M. A. Hanninglee, A. Biswas, A. E. Stiegman, G. W. Scott, *J. Am. Chem. Soc.* **1995**, *117*, 2618. b) K. Tran, A. E. Stiegman, G. W. Scott, *Inorg. Chim. Acta* **1996**, *243*, 185.
19 S. Yoshida, Y. Magatani, S. Noda, T. Funabiki, *Chem. Commun.* **1981**, 601. b) S. Yoshida, T. Tanaka, M. Okada, T. Funabiki, *J. Chem. Soc., Faraday Trans.* **1984**, *80*, 119.
20 T. Tanaka, M. Ooe, T. Funabiki, S. Yoshida, *J. Chem. Soc., Faraday Trans.* **1986**, *82*, 35.
21 a) H. Yoshida, T. Tanaka, M. Yamamoto, T. Funabiki, S. Yoshida, *Chem. Commun.* **1996**, 2125. b) H. Yoshida, T. Tanaka, M. Yamamoto, T. Yoshida, T. Funabiki, S. Yoshida, *J. Catal.* **1997**, *171*, 351.
22 F. Amano, T. Tanaka, T. Funabiki, *Langmuir* **2004**, *20*, 4236.
23 F. Amano, T. Tanaka, *Catal. Commun.* **2005**, *6*, 269.
24 F. Amano, T. Yamaguchi, T. Tanaka, *J. Phys. Chem. B* **2006**, *110*, 281.
25 T. Yamamoto, T. Tanaka, T. Funabiki, S. Yoshida, *J. Phys. Chem. B* **1998**, *102*, 5830.
26 a) H. Yamashita, K. Yoshizawa, M. Ariyuki, S. Higashimoto, M. Che, M. Anpo, *Chem. Commun.* **2001**, 435. b) Y. Shiraishi, Y. Teshima, T. Hirai, *Chem. Commun.* **2005**, 4569.
27 T. Tanaka, Y. Nishimura, S. Kawasaki, M. Ooe, T. Funabiki, S. Yoshida, *J. Catal.* **1989**, *118*, 327.
28 a) T. Tanaka, S. Takenaka, T. Funabiki, S. Yoshida, *Chem. Lett.* **1994**, 1585. b) S. Takenaka, T. Kuriyama, T. Tanaka, T. Funabiki, S. Yoshida, *J. Catal.* **1995**, *155*, 196. c) T. Tanaka, S. Takenaka, T. Funabiki, S. Yoshida, *J. Chem. Soc., Faraday Trans.* **1996**, *92*, 1975. d) S. Takenaka, T. Tanaka, T. Funabiki, S. Yoshida, *Catal. Lett.* **1997**, *44*, 67.
29 S. Yoshida, T. Tanaka, Y. Nishimura, H. Mizutani, T. Funabiki, *Proc.-Int. Congr. Catal., 9th* **1988**, *3*, 1473.
30 X. T. Gao, S. R. Bare, B. M. Weckhuysen, I. E. Wachs, *J. Phys. Chem. B* **1998**, *102*, 10842.
31 S. Takenaka, T. Tanaka, T. Yamazaki, T. Funabiki, S. Yoshida, *J. Phys. Chem. B* **1997**, *101*, 9035.
32 a) K. Wada, M. Nakashita, A. Yamamoto, T. Mitsudo, *Chem. Commun.* **1998**, 133. b) K. Wada, H. Yamada, E. Watanabe, T. Mitsudo, *J. Chem. Soc., Faraday Trans.* **1998**, *94*, 1771.
33 a) K. Teramura, T. Tanaka, T. Yamamoto, T. Funabiki, *J. Mol. Catal. A: Chem.* **2001**, *165*, 299. b) K. Teramura, T. Tanaka, M. Kani, T. Hosokawa, T. Funabiki, *J. Mol. Catal. A: Chem.* **2004**, *208*, 299.
34 S. Takenaka, T. Tanaka, T. Funabiki, S. Yoshida, *J. Chem. Soc., Faraday Trans.* **1997**, *93*, 4151.
35 F. Amano, T. Ito, S. Takenaka, T. Tanaka, *J. Phys. Chem. B* **2005**, *109*, 10973.
36 T. Tanaka, T. Ito, S. Takenaka, T. Funabiki, S. Yoshida, *Catal. Today* **2000**, *61*, 109.